THE JOURNAL OF PHYSICAL CHEMISTRY Letters

LETTER

pubs.acs.org/JPCL

A High Yield Synthesis of Ligand-Free Iridium Oxide Nanoparticles with High Electrocatalytic Activity

Yixin Zhao, Emil A. Hernandez-Pagan, Nella M. Vargas-Barbosa, Jennifer L. Dysart, and Thomas E. Mallouk*

Department of Chemistry, The Pennsylvania State University, University Park, Pennsylvania, 16802, United States

Supporting Information

ABSTRACT: Stable blue suspensions of 2 nm diameter iridium oxide ($IrO_x \cdot nH_2O$) nanoparticles were obtained by hydrolyzing $IrCl_6^{2-}$ in base at 90 °C to produce $[Ir(OH)_6]^{2-}$ and then treating with HNO_3 at 0 °C. UV−visible spectra show that acid condensation of $[Ir(OH)_6]^{2-}$ results in quantitative conversion to stable, ligand-free $IrO_x \cdot nH_2O$ nanoparticles, which have an extinction coefficient of 630 ± 50 $M^{-1}cm^{-1}$ at 580 nm. In contrast, alkaline hydrolysis alone converts only 30% of the sample to $IrO_x \cdot nH_2O$ at 2 mM concentration. The acidified nanoparticles are stable for at least one month at 2 °C and can be used to make colloidal solutions between pH 1 and 13. At pH 7 and above, some hydrolysis to form $[Ir(OH)_6]^{2-}$ occurs. Uniform $IrO_x \cdot nH_2O$ electrode films were grown anodically from pH 1 solutions, and were found to be highly active for water oxidation between pH 1 and 13.

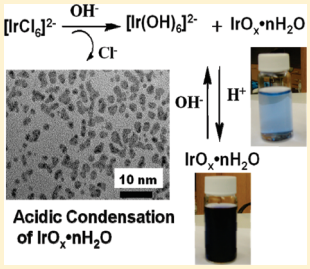

SECTION: Nanoparticles and Nanostructures

Recent research activity in artificial photosynthesis has intensified the search for water oxidation catalysts that can function at high turnover rates and low overpotentials.[1−15] Despite the high cost and low terrestrial abundance of iridium, hydrated iridium oxide ($IrO_x \cdot nH_2O$) has been useful for fundamental studies of the water splitting reaction because it can be made as stable nanoparticles, and because it is highly active for water oxidation over a broad range of pH.[16−26] The synthesis of $IrO_x \cdot nH_2O$ colloids was first reported over 100 years ago,[27] and that synthetic method (alkaline hydrolysis of $[IrCl_6]^{2-}$) produces blue colloids with particle sizes in the 1−2 nm range. Recently, Murray and co-workers used this method to deposit electrode films of $IrO_x \cdot nH_2O$, which they showed are very good electrocatalysts over a broad range of pH.[22,28] Alternative syntheses of $IrO_x \cdot nH_2O$ colloids have used stabilizing ligands with multiple carboxylate groups, such as malonate or succinate.[29−32] With these stabilizing ligands, the colloids may be incorporated into photoelectrodes and other assemblies for overall light-driven water splitting.[23,33−35] In syntheses using capping ligands, the yield of stable colloid is rarely quantitative, and some of the $IrO_x \cdot nH_2O$ precipitates as large particles. Similarly, in our hands the alkaline route to uncapped colloids gives solutions of varying color, from pale to deep blue. Another complication of current synthetic methods is that $IrO_x \cdot nH_2O$ nanoparticles are not stable under acidic conditions; for example citrate-capped $IrO_x \cdot nH_2O$ precipitates at pH < 3,[36] and ligand-free $IrO_x \cdot nH_2O$ nanoparticles synthesized by alkaline hydrolysis are unstable at neutral pH.[22] Because of these problems, we have conducted a study of the alkaline hydrolysis process, the results of which are reported here. We identify conditions for obtaining quantitative yields of catalytically active, uncapped colloids that are stable over a wide range of pH.

Hydrolysis of K_2IrCl_6. Both bulk and colloidal Ir(IV) oxides show a characteristic absorbance peak at about 580 nm, whereas the monomeric $[Ir(OH)_6]^{2-}$ complex has no visible absorbance and a strong UV band at 313 nm.[37,38] By monitoring the UV−visible spectrum, one can follow the formation of $IrO_x \cdot nH_2O$ from K_2IrCl_6 through $[Ir(OH)_6]^{2-}$. The condensation reaction of $[Ir(OH)_6]^{2-}$ to form $IrO_x \cdot nH_2O$ nanoparticles has not been studied systematically, although Harriman and co-workers have noted the $[Ir(OH)_6]^{2-}$ intermediate in the radiolytic conversion of $[IrCl_6]^{3-}$ to $IrO_x \cdot nH_2O$.[16,19] Because one can expect the condensation reaction to be concentration-dependent, we recorded UV−visible spectra at high (2 mM) and low (0.10−0.15 mM) concentrations over a range of pH and heating conditions.

The electronic spectra of red-brown K_2IrCl_6 solutions in water, adjusted to pH 13 but not heated, are shown in Figure 1A. Both the 0.1 mM and 2 mM solutions have strong visible bands that disappear as the solution is heated briefly to 50 °C, as shown in Figure 1B−C. The disappearance of these visible bands and appearance of the strong absorption at 313 nm can be attributed to hydrolysis of the Ir−Cl bonds and formation of the yellow $[Ir(OH)_6]^{2-}$ complex. The UV absorbance grows progressively as the solution is heated to higher temperature, showing that the hydrolysis reaction is not complete until the solution is heated above about 70−80 °C. Interestingly, the 580 nm band begins to appear only after heating to 90 °C in the case of the 2 mM solution, and is completely suppressed in the more dilute solution (Figure 1C). These observations signal a slow, concentration-dependent condensation reaction of $[Ir(OH)_6]^{2-}$ to form

Received: January 11, 2011
Accepted: January 27, 2011

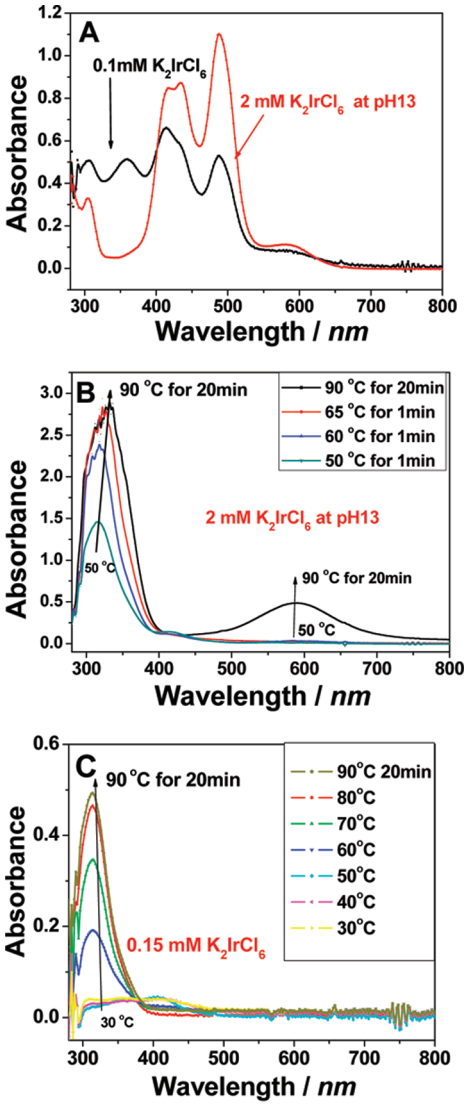

Figure 1. UV−visible spectra of (A) unheated 0.1 mM and 2 mM aqueous K_2IrCl_6 solutions at pH 13; (B) 2 mM K_2IrCl_6 heated at pH 13 to 50, 60, and 65 °C for 1 min, and the same solution after heating to 90 °C for 20 min; (C) 0.15 mM K_2IrCl_6 at pH 13 after heating to 30, 40, 50, 60, 70, and 80 °C, and finally after holding at 90 °C for 20 min.

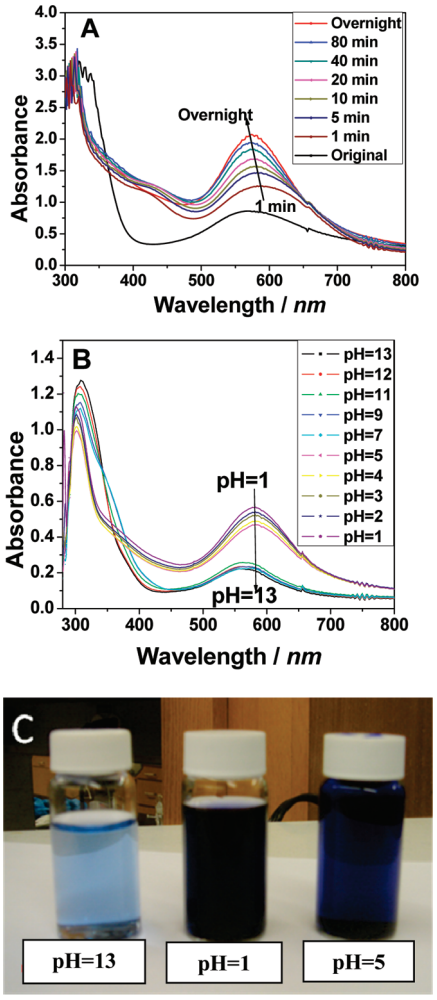

Figure 2. UV−visible spectra of (A) $IrO_x \cdot nH_2O$ solution prepared from 2 mM pH 13 Ir(IV) solutions, after adjusting the pH to 1 by addition of 3 M HNO_3 at ice temperature. Spectra are shown after different reaction times. (B) Acid-treated $IrO_x \cdot nH_2O$ solutions adjusted to pH 1−13 by addition of NaOH; (C) Photographs of an Ir(IV) solution prepared by hydrolysis at pH 13 (90 °C, 20 min) (left), the same solution after reaction with HNO_3 (center) and then adjusting to pH 5 by addition of NaOH (right).

$IrO_x \cdot nH_2O$ colloids. The persistence of the intense UV band in the 2 mM solution shows that at this concentration, relatively little of the Ir(IV) is converted to the blue colloid. This is consistent with the batch-to-batch variability of colloids prepared by alkaline hydrolysis.

Acidic Condensation of $IrO_x \cdot nH_2O$. When 1 mL of 3 M HNO_3 solution was rapidly added to 50 mL of rapidly stirred, ice cold Ir(IV) solutions (prepared from 2 mM pH 13 K_2IrCl_6, which had been heated at 90 °C for 20 min), the color of the solution changed progressively from blue to purple blue, green, and then deep dark blue. The initial color changes occurred very rapidly, and the final blue color then became deeper with time (on a time scale of minutes to hours) as shown in Figure 2A. The strong UV band associated with monomeric $[Ir(OH)_6]^{2-}$ disappeared rapidly. Early in the reaction, a band at 420 nm appeared, which then broadened and decreased in intensity on a time scale of hours. This progression of spectral changes is consistent with protonation and rapid condensation of $[Ir(OH)_6]^{2-}$ to form $Ir^{IV}-O-Ir^{IV}$ linkages, which give rise to the absorption at 580 nm. The gradual disappearance of the 420 nm band appears to signal a slower condensation step as Ir−O−Ir bonds are formed within the nanoparticles. Residual absorbance in the range of 300−310 nm could be attributed to HNO_3 (this was confirmed in a blank experiment). This conclusion was also confirmed by carrying out the acid condensation reaction with HBF_4 in place of HNO_3 (see Supporting Information). From these data we were able to calculate extinction coefficients of 3370 ± 10 and 630 ± 50 for $[Ir(OH)_6]^{2-}$ at 313 nm and acidic $IrO_x \cdot nH_2O$ at 574 nm, respectively. From these extinction coefficients, we estimate that alkaline hydrolysis converts only about 30% of the sample to $IrO_x \cdot nH_2O$ at 2 mM concentration.

When the acid condensation reaction was carried out at ice temperature, no precipitate formed, and the blue colloidal solutions were stable for at least 1 month at 2 °C. Transmission electron microscopy (TEM) images (see Supporting Information) showed irregularly shaped, isolated particles in the range of 1−4 nm diameter with a mean diameter of 2 nm. If the

Scheme 1. Proposed Growth Mechanism for the Basic Hydrolysis of $[IrCl_6]^{2-}$ Ions and Acid Condensation of Ligand-Free $IrO_x \cdot nH_2O$ Nanoparticles

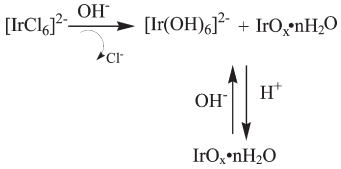

$IrO_x \cdot nH_2O$ solution was not kept cold, a significant quantity of blue precipitate formed when the HNO_3 was added, but a clear deep blue solution was obtained after the precipitate was removed by filtration or centrifugation.

$IrO_x \cdot nH_2O$ colloids do not precipitate from cold solutions when the pH is adjusted between pH 1 and 13 by adding NaOH solution, as shown in Figure 2B,C. The absorbance at 580 nm decreases with increasing pH, with an abrupt change between pH 5 and 7. As the solution is made more basic, the 580 nm absorption band decreases in intensity and it shifts to shorter wavelength. At the same time, the strong UV band reappears. These spectral changes, which are apparent in the colors of the colloidal solutions (Figure 2C), suggest that some but not all of the colloid is hydrolyzed to $[Ir(OH)_6]^{2-}$ in basic solutions. A sequence of reactions that is consistent with these spectral changes is shown in Scheme 1. $[IrCl_6]^{2-}$ ions are first hydrolyzed to $[Ir(OH)_6]^{2-}$ by heating in base; the $[Ir(OH)_6]^{2-}$ monomers, at sufficiently high concentration, partially polymerize to form $IrO_x \cdot nH_2O$, which is stabilized by OH^- groups. Protonation of these anionic clusters results in aggregation and condensation with $[Ir(OH)_6]^{2-}$, which is also protonated in the reaction. The slow condensation that results in the formation of $IrO_x \cdot nH_2O$ nanoparticles can be partially reversed by addition of base to form $[Ir(OH)_6]^{2-}$.

Electrochemical Activity. The $IrO_x \cdot nH_2O$ nanoparticles was deposited on glassy carbon electrodes by applying +1.4 V versus AgCl/Ag for 15 min, as described in previous reports.[22,28,39,40] Under alkaline conditions, the deposition reaction has been attributed to electro-flocculation, which is driven by the generation of protons in the water oxidation reaction.[22] Using this technique, it is difficult to fabricate uniform $IrO_x \cdot nH_2O$ thin films on fluorine-doped tin oxide (FTO) electrodes, and precipitates also form in the solution around the electrode. Using acidic colloidal solutions, uniform films could be grown as confirmed by scanning electron microscopy (SEM) and optical microscopy (see Supporting Information), and no precipitate formed in the solution. The mechanism for anodic deposition of ligand-free $IrO_x \cdot nH_2O$ may be similar to that previously reported for assembly of citrate-capped $IrO_x \cdot nH_2O$ colloids on FTO electrodes.[36,41] Rotating disk electrode (RDE) experiments with glassy carbon electrodes gave results that were similar to those reported by Murray et al. (see Supporting Information), but with ~30 mV lower overpotential for oxygen evolution (0.22 V at 0.5 mA/cm^2 current density) across the pH range 1−13. We tentatively ascribe the improved performance of these electrodes to higher utilization of Ir(IV) using the acidic condensation method. The coverage of electroactive Ir(IV), Γ_{Ir}, calculated by integration of the Ir^V/Ir^{IV} wave, was 1.1×10^{-8} mol/cm^2 at pH 1, and the current density for water oxidation at 1.4 V versus AgCl/Ag at pH 1 was 20 mA/cm^2. This is significantly higher than the previously reported current density at the same potential obtained with a thicker film (Γ_{Ir} 7.8×10^{-8} mol/cm^2) of nanoparticles made by alkaline hydrolysis.[22] We found Γ_{Ir} of IrO_x thin films in pH 13 solutions to be about 1/3 that in pH 1 solutions, even though the films were grown from the same solutions under the same deposition conditions. The significant decrease in Γ_{Ir} at pH 13 may result from the dissolution of the colloid, as observed in the UV−visible study (Figure 2B).

Solutions of ligand-free $IrO_x \cdot nH_2O$ nanoparticles were made in a two-step process of alkaline hydrolysis and acidic condensation. This procedure results in a reproducibly high yield of stable colloid from soluble precursors. The acidic $IrO_x \cdot nH_2O$ colloids if kept cold have good stability in both acidic and basic solutions. These nanoparticles can be deposited anodically on electrodes as uniform thin films and show current densities comparable to the highest reported values. Preliminary experiments show that these uncapped nanoparticles can be coordinated by free malonate ligands and they are thus good candidates for incorporating into molecular assemblies for photoelectrochemical water splitting. Experiments along these lines are currently in progress.

EXPERIMENTAL DETAILS

Preparation of $IrO_x \cdot nH_2O$ Nanoparticles in Acidic Solution. Fifty milliliters of 2.0 mM aqueous K_2IrCl_6 solution was adjusted to pH 13 (similar results were obtained from pH 12−14) with 10 wt % aqueous NaOH to obtain a yellow solution, which was then heated at 90 °C for 20 min as described in previous reports.[22,28] The resulting solutions, which were kept in an ice bath, had a blue color with different absorbance values from batch to batch. The cold solution was adjusted to pH 1 by rapidly adding 3 M HNO_3 and was stirred continuously for 80 min until the solution became deep blue. The solution was then stored in a refrigerator at 2 °C. The solution was adjusted as desired to pH 1−13 by addition of dilute 1.5 wt % NaOH solution.

Electrochemical Measurements. All electrochemical measurements and colloid deposition were performed with a BAS 100B electrochemical workstation. $IrO_x \cdot nH_2O$ nanoparticle films were deposited on glassy carbon, gold, and FTO-coated glass electrodes using a pH 1 $IrO_x \cdot nH_2O$ solution at a potential of +1.4 V versus Ag/AgCl, NaCl (3 M) for different periods of time. The acidic $IrO_x \cdot nH_2O$ nanoparticles deposited on glassy carbon RDEs (5 mm diameter) were tested in the following solutions: pH 1 H_2SO_4 solution [0.098 M] containing 0.1 M Na_2SO_4; pH 4.5 and 9 phosphate [0.1 M] buffer solutions containing 0.1 M Na_2SO_4; pH 5.7 solution containing 0.0375 M Na_2SiF_6, 0.056 M $NaHCO_3$, and 0.1 M Na_2SO_4; and pH 13 NaOH solution [0.1M] containing 0.1 M Na_2SO_4.

Characterization. UV−visible spectra were recorded on a HP 8452A diode array spectrophotometer. $IrO_x \cdot nH_2O$ nanoparticles and films were imaged by SEM (FESEM, JEOL JSM 4700F) and high-resolution TEM (Philips EM420T).

ASSOCIATED CONTENT

Supporting Information. UV−visible spectra of acidic $IrO_x \cdot nH_2O$ colloids prepared using HBF_4 and HCl in place of HNO_3, TEM images of $IrO_x \cdot nH_2O$ nanoparticles, photographs of FTO electrodes with colloidal $IrO_x \cdot nH_2O$ films, and electrochemical data from RDE experiments (5 pp). This material is available free of charge via the Internet at http://pubs.acs.org.

AUTHOR INFORMATION

Corresponding Author
*E-mail: tem5@psu.edu.

ACKNOWLEDGMENT

This work was supported by the Office of Basic Energy Sciences, Division of Chemical Sciences, Geosciences, and Energy Biosciences, Department of Energy, under Contract DE-FG02-07ER15911.

REFERENCES

(1) Blakemore, J. D.; Schley, N. D.; Balcells, D.; Hull, J. F.; Olack, G. W.; Incarvito, C. D.; Eisenstein, O.; Brudvig, G. W.; Crabtree, R. H. Half-Sandwich Iridium Complexes for Homogeneous Water-Oxidation Catalysis. *J. Am. Chem. Soc.* **2010**, *132*, 16017–16029.

(2) Brimblecombe, R.; Swiegers, G. F.; Dismukes, G. C.; Spiccia, L. Sustained Water Oxidation Photocatalysis by a Bioinspired Manganese Cluster. *Angew. Chem., Int. Ed.* **2008**, *47*, 7335–7338.

(3) Chen, H. Y.; Faller, J. W.; Crabtree, R. H.; Brudvig, G. W. Dimer-of-Dimers Model for the Oxygen-Evolving Complex of Photosystem II. Synthesis and Properties of $[Mn^{IV}{}_4O_5(terpy)_4(H_2O)_2](ClO_4)_6$. *J. Am. Chem. Soc.* **2004**, *126*, 7345–7349.

(4) Concepcion, J. J.; Jurss, J. W.; Templeton, J. L.; Meyer, T. J. Mediator-Assisted Water Oxidation by the Ruthenium "Blue Dimer" *cis, cis*-$[(bpy)_2(H_2O)RuORu(OH_2)(bpy)_2]^{4+}$. *Proc. Natl. Acad. Sci. U.S.A.* **2008**, *105*, 17632–17635.

(5) Dinca, M.; Surendranath, Y.; Nocera, D. G. Nickel-Borate Oxygen-Evolving Catalyst that Functions under Benign Conditions. *Proc. Natl. Acad. Sci. U.S.A.* **2010**, *107*, 10337–10341.

(6) Geletii, Y. V.; Huang, Z. Q.; Hou, Y.; Musaev, D. G.; Lian, T. Q.; Hill, C. L. Homogeneous Light-Driven Water Oxidation Catalyzed by a Tetraruthenium Complex with All Inorganic Ligands. *J. Am. Chem. Soc.* **2009**, *131*, 7522–7523.

(7) Hurst, J. K.; Cape, J. L.; Clark, A. E.; Das, S.; Qin, C. Y. Mechanisms of Water Oxidation Catalyzed by Ruthenium Diimine Complexes. *Inorg. Chem.* **2008**, *47*, 1753–1764.

(8) Jiao, F.; Frei, H. Nanostructured Manganese Oxide Clusters Supported on Mesoporous Silica as Efficient Oxygen-Evolving Catalysts. *Chem. Commun.* **2010**, *46*, 2920–2922.

(9) Kanan, M. W.; Nocera, D. G. In Situ Formation of an Oxygen-Evolving Catalyst in Neutral Water Containing Phosphate and Co^{2+}. *Science* **2008**, *321*, 1072–1075.

(10) McDaniel, N. D.; Coughlin, F. J.; Tinker, L. L.; Bernhard, S. Cyclometalated Iridium(III) Aquo Complexes: Efficient and Ttunable Catalysts for the Homogeneous Oxidation of Water. *J. Am. Chem. Soc.* **2008**, *130*, 210–217.

(11) Somorjai, G. A.; Frei, H.; Park, J. Y. Advancing the Frontiers in Nanocatalysis, Biointerfaces, and Renewable Energy Conversion by Innovations of Surface Techniques. *J. Am. Chem. Soc.* **2009**, *131*, 16589–16605.

(12) Xu, Y. H.; Duan, L. L.; Tong, L. P.; Akemark, B.; Sun, L. C. Visible Light-Driven Water Oxidation by a Highly Efficient Dinuclear Ruthenium Complex. *Chem. Commun.* **2010**, *46*, 6506–6508.

(13) Yin, Q. S.; Tan, J. M.; Besson, C.; Geletii, Y. V.; Musaev, D. G.; Kuznetsov, A. E.; Luo, Z.; Hardcastle, K. I.; Hill, C. L. A Fast Soluble Carbon-Free Molecular Water Oxidation Catalyst Based on Abundant Metals. *Science* **2010**, *328*, 342–345.

(14) Zong, R.; Thummel, R. P. A New Family of Ru Complexes for Water Oxidation. *J. Am. Chem. Soc.* **2005**, *127*, 12802–12803.

(15) Geletii, Y. V.; Botar, B.; Koegerler, P.; Hillesheim, D. A.; Musaev, D. G.; Hill, C. L. An All-Inorganic, Stable, and Highly Active Tetraruthenium Homogeneous Catalyst for Water Oxidation. *Angew. Chem., Int. Ed.* **2008**, *47*, 3896–3899.

(16) Han, H. X.; Frei, H. Controlled Assembly of Hetero-binuclear Sites on Mesoporous Silica: Visible Light Charge-Transfer Units with Selectable Redox Properties. *J. Phys. Chem. C* **2008**, *112*, 8391–8399.

(17) Harriman, A.; Nahor, G. S.; Mosseri, S.; Neta, P. Iridium Oxide Hydrosols as Catalysts for the Decay of Zinc Porphyrin Radical Cations in Water. *J. Chem. Soc., Faraday Trans.* **1988**, *84*, 2821–2829.

(18) Harriman, A.; Thomas, J. M.; Millward, G. R. Catalytic and Structural-Properties of Iridium-Iridium Dioxide Colloids. *New J. Chem.* **1987**, *11*, 757–762.

(19) Morris, N. D.; Mallouk, T. E. A High-Throughput Optical Screening Method for the Optimization of Colloidal Water Oxidation Catalysts. *J. Am. Chem. Soc.* **2002**, *124*, 11114–11121.

(20) Nahor, G. S.; Hapiot, P.; Neta, P.; Harriman, A. Changes in the Redox State of Iridium Oxide Clusters and Their Relation to Catalytic Water Oxidation. Radiolytic and Electrochemical Studies. *J. Phys. Chem.* **1991**, *95*, 616–621.

(21) Nahor, G. S.; Neta, P.; Hambright, P.; Thompson, A. N.; Harriman, A. Metalloporphyrin-Sensitized Photooxidation of Water to Oxygen on the Surface of Colloidal Iridium Oxides. Photochemical and Pulse Radiolytic Studies. *J. Phys. Chem.* **1989**, *93*, 6181–6187.

(22) Nakagawa, T.; Beasley, C. A.; Murray, R. W. Efficient Electro-Oxidation of Water near Its Reversible Potential by a Mesoporous IrOx Nanoparticle Film. *J. Phys. Chem. C* **2009**, *113*, 12958–12961.

(23) Nakamura, R.; Frei, H. Visible Light-Driven Water Oxidation by Ir Oxide Clusters Coupled to Single Cr Centers in Mesoporous Silica. *J. Am. Chem. Soc.* **2006**, *128*, 10668–10669.

(24) Yagi, M.; Tomita, E.; Kuwabara, T. Remarkably High Activity of Electrodeposited IrO_2 Film for Electrocatalytic Water Oxidation. *J. Electroanal. Chem.* **2005**, *579*, 83–88.

(25) Youngblood, W. J.; Lee, S. H. A.; Kobayashi, Y.; Hernandez-Pagan, E. A.; Hoertz, P. G.; Moore, T. A.; Moore, A. L.; Gust, D.; Mallouk, T. E. Photoassisted Overall Water Splitting in a Visible Light-Absorbing Dye-Sensitized Photoelectrochemical Cell. *J. Am. Chem. Soc.* **2009**, *131*, 926–927.

(26) Youngblood, W. J.; Lee, S. H. A.; Maeda, K.; Mallouk, T. E. Visible Light Water Splitting Using Dye-Sensitized Oxide Semiconductors. *Acc. Chem. Res.* **2009**, *42*, 1966–1973.

(27) Wohler, L.; Witzmann, W. Z. Die Oxyde des Iridiums. *Anorg. Chem.* **1908**, *57*, 323–352.

(28) Nakagawa, T.; Bjorge, N. S.; Murray, R. W. Electrogenerated IrO_x Nanoparticles as Dissolved Redox Catalysts for Water Oxidation. *J. Am. Chem. Soc.* **2009**, *131*, 15578–15579.

(29) Hara, M.; Lean, J. T.; Mallouk, T. E. Photocatalytic Oxidation of Water by Silica-Supported Tris(4,4′-dialkyl-2,2′-bipyridyl)ruthenium Polymeric Sensitizers and Colloidal Iridium Oxide. *Chem. Mater.* **2001**, *13*, 4668–4675.

(30) Hara, M.; Mallouk, T. E. Photocatalytic Water Oxidation by Nafion-Stabilized Iridium Oxide Colloids. *Chem. Commun.* **2000**, 1903–1904.

(31) Hara, M.; Waraksa, C. C.; Lean, J. T.; Lewis, B. A.; Mallouk, T. E. Photocatalytic Water Oxidation in a Buffered Tris(2,2′-bipyridyl)ruthenium Complex−Colloidal IrO_2 System. *J. Phys. Chem. A* **2000**, *104*, 5275–5280.

(32) Hoertz, P. G.; Kim, Y. I.; Youngblood, W. J.; Mallouk, T. E. Bidentate Dicarboxylate Capping Groups and Photosensitizers Control the Size of IrO_2 Nanoparticle Catalysts for Water Oxidation. *J. Phys. Chem. B* **2007**, *111*, 6845–6856.

(33) Brimblecombe, R.; Koo, A.; Dismukes, G. C.; Swiegers, G. F.; Spiccia, L. Solar Driven Water Oxidation by a Bioinspired Manganese Molecular Catalyst. *J. Am. Chem. Soc.* **2010**, *132*, 2892–2893.

(34) Kim, W.; Tachikawa, T.; Majima, T.; Li, C.; Kim, H. J.; Choi, W. Tin Porphyrin Sensitized TiO_2 for the Production of H_2 Under Visible Light. *Energy Environ. Sci.* **2010**, *3*, 1789–1795.

(35) Li, L.; Duan, L. L.; Xu, Y. H.; Gorlov, M.; Hagfeldt, A.; Sun, L. C. A Photoelectrochemical Device for Visible Light Driven Water Splitting by a Molecular Ruthenium Catalyst Assembled on Dye-Sensitized Nanostructured TiO_2. *Chem. Commun.* **2010**, *46*, 7307–7309.

(36) Kuwabara, T.; Tomita, E.; Sakita, S.; Hasegawa, D.; Sone, K.; Yagi, M. Characterization and Analysis of Self-Aassembly of a Highly Active Colloidal Catalyst for Water Oxidation onto Transparent Conducting Oxide Substrates. *J. Phys. Chem. C* **2008**, *112*, 3774–3779.

(37) Desideri, P. G.; Pantani, F. *Ric. Sci., Parte 2: Rend.* **1961**, *1*, 265.

(38) van Loon, G.; Page, J. A. The Chemistry of Iridium in Basic Aqueous Solution: A Polarographic Study. *Can. J. Chem.* **1966**, *44*, 515–520.

(39) Hu, J.; Abdelsalam, M.; Bartlett, P.; Cole, R.; Sugawara, Y.; Baumberg, J.; Mahajan, S.; Denuault, G. Electrodeposition of Highly Ordered Macroporous Iridium Oxide through Self-Assembled Colloidal Templates. *J. Mater. Chem.* **2009**, *19*, 3855–3858.

(40) Petit, M. A.; Plichon, V. Anodic Electrodeposition of Iridium Oxide Films. *J. Electroanal. Chem.* **1998**, *444*, 247–252.

(41) Yagi, M.; Tomita, E.; Sakita, S.; Kuwabara, T.; Nagai, K. Self-Assembly of Active IrO_2 Colloid Catalyst on an ITO Electrode for Efficient Electrochemical Water Oxidation. *J. Phys. Chem. B* **2005**, *109*, 21489–21491.